bution patterns, we find that the qualitative nature of fly ash as independent of coal source and firing conditions. This suggests that the ashes are in near-equilibrium states rather than as frozen transients. Growth of the mullite crystallites occurs over several micrometers (Fig. 1). This means that there was time for the trace elements to be frozen out and concentrated in the glass phases. Perhaps the segregation of trace elements at fly ash surfaces, reported by Linton *et al.* (*3*) and Smith *et al.* (*4*), occurs by transport from the inside of the particle as well as by condensation from the vapor phase. The Gibbs adsorption isotherm states that the surface free energy of liquids decreases when solutes migrate to the surface. Long-term leaching behavior occurs primarily in glass and magnetic spinel matrices. It appears to us that, if the magnetic phases are removed from fly ash specimens before they are buried, the amount of leaching and runoff from first-row transition elements would diminish. Pollution from Cr and Ni should be especially reduced. The Cr in the nonmagnetic phase is trapped in the mullite lattice that should be more inert to breakdown. It appears to us that the mullite and quartz present in fly ash may be a valuable resource. As much as 30 percent of the nonmagnetic fraction is in this form. Mullite is a widely marketed refractory ceramic used for making china, electrical insulators, and high-temperature devices. Mullite is presently made by the mining and firing of kaolinite, which is an energy-intensive process. Perhaps the chemical refinement of mullite and quartz already present in fly ash has economic merit.

L. D. HULETT, JR., A. J. WEINBERGER
K. J. NORTHCUTT, MARIAN FERGUSON
Oak Ridge National Laboratory,
Oak Ridge, Tennessee 37830

References and Notes

1. L. D. Hulett and A. J. Weinberger, *Environ. Sci. Technol.* **14**, 965 (1980).
2. _____, N. M. Ferguson, K. J. Northcutt, W. S. Lyon, Report RP 1061 (Electric Power Research Institute, Palo Alto, Calif., July 1979).
3. R. W. Linton, P. Williams, C. A. Evans, D. F. S. Natusch, *Anal. Chem.* **49**, 1514 (1977).
4. R. D. Smith, J. A. Campbell, K. K. Nielson, *J. Am. Chem. Soc.* **13**, 553 (1979).
5. We thank the Tennessee Valley Authority for supplying ash samples. We appreciate the expert guidance in photography given by J. W. Jones. Research supported by the Electric Power Research Institute, Palo Alto, Calif.

14 February 1980; revised 14 July 1980

Resonance Raman Effect of Carbonyl Group as a Probe of Its π-Electron State

Abstract. *By examining the occurrence or absence of a resonance Raman effect for a carbonyl bond-stretching vibration, one can achieve a unique characterization of the carbonyl π-electrons. It can be concluded, for example, that the carbonyl π-electrons of nicotinamide do not migrate into the ring π-electron orbitals responsible for the 265-nanometer band, whereas those of dihydronicotinamide do migrate into orbitals responsible for the 340-nanometer band.*

The Raman line caused by a carbonyl stretching vibration is often strong and is usually identified with high reliability, even in a complex compound such as a nucleic acid, a coenzyme, or an antibiotic. The question may be raised, Under what condition is a carbonyl stretching vibration involved in a resonance Raman effect? As an answer we suggest a simple rule: A carbonyl stretching vibration will show greatly enhanced intensity in a resonance Raman spectrum from a given excited electronic state if the state is a $\pi\pi^*$ transition of a conjugated double-bond system and if the carbonyl bond in question is involved in the conjugated system.

This rule is an extension of one published by Hirakawa and Tsuboi (*1*), which stated that, if there is a change in the molecular geometry in the excited electronic state that mirrors a normal mode of the ground-state molecule, then that normal mode will be active in the resonance Raman spectrum. In the present case, if the π-electrons in the carbonyl bond are involved in the electronic transition, there will be a decrease in the bond order of the carbonyl bond and consequently a lengthening of that bond. We will review experimental evidence for the rule and give some examples to show how it is useful in the present, less general form.

Our experimental results are summarized in Table 1. A resonance Raman effect is most reliably detected by examination of a Raman excitation profile. If, in a curve of the intensity I_j of a Raman line j plotted against the excitation wavelength λ_{exc}, a peak appears in an absorption band $\tilde{N} \leftarrow \tilde{X}$, it is concluded that j is in resonance with $\tilde{N} \leftarrow \tilde{X}$. The same conclusion is often drawn merely by observing a well-defined Raman line with an excitation wavelength in the $\tilde{N} \leftarrow \tilde{X}$ band. If the molar extinction coefficient for λ_{exc} is 10^3 to 10^4, the sample concentration (in an aqueous solution, for example) for the Raman scattering measurement is usually 10^{-3} to $10^{-4}M$. The fact that a distinct Raman line is observed for such a dilute sample solution is taken as an evidence of the resonance Raman effect.

In acrolein (**1**), the Raman scattering intensity of the C=O stretching vibration at 1693 cm^{-1} increases monotonously on changing λ_{exc} from 363.8 to 290 nm. It is concluded that the C=O Raman line is not in resonance with the 340-nm band [$n\pi^*$ transition of the O=C-C=C system (*2*)], but it probably is in resonance with the 197-nm band ($\pi\pi^*$ transition). The 250-nm band of thiourea (**2**) is essentially the longest wavelength $\pi\pi^*$ transition (*3*), and the C=S stretching Raman line is in resonance with this band (*4*). The uracil residue (**3**) has two C=O stretching vibrations. The 1720-cm^{-1} line (C^2=O) is not in resonance with the 260-nm band, whereas the 1680-cm^{-1} line (C^4=O) is in resonance (*5*). The electrons associated with the 260-nm band ($\pi\pi^*$) are known to be localized in the O=C^4-C^5=C^6 part of the molecule, and the C^2=O bond is not considered to be involved in the conjugated double-bond system (*6*, *7*). These observations are considered to form evidence for the rule stated above. This interpretation is supported by the fact that the 4-thiouracil residue (**4**) has a C=O stretching vibration (1700 cm^{-1}) that is not in resonance with its 333-nm band, whereas the 2-thiouracil residue (**5**) has a C=O Raman line (1690 cm^{-1}) that is in resonance with its 300-nm band.

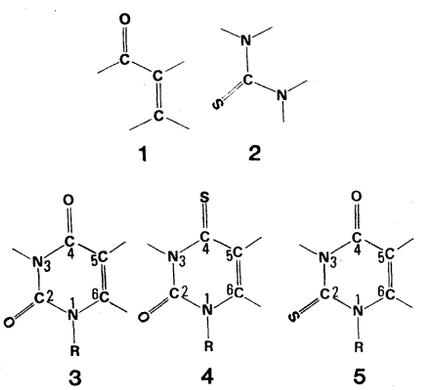

The rule can be used to judge whether a particular carbonyl group is involved in a conjugated double-bond system. Even when a C=O bond appears, from the structural formula, to be conjugated with a C=C (or C=N) bond, the π-electrons

0036-8075/80/1219-1358$00.50/0

Table 1. Occurrence of resonance Raman effects in some carbonyl stretching vibrations.

Carbonyl compound	Absorption band (nm)	Carbonyl stretching vibration	(cm^{-1})	λ_{exc} (nm)	Resonance
(1) Acrolein	340	C=O	1693	300, 290	No
(2) Thiourea	250	C=S	729	257.3	Yes
(3) Uracil residue	260	C^2=O	1720	257.3	No
		C^4=O	1680	257.3	Yes
(4) 4-Thiouracil residue	333	C^2=O	1700	363.8	No
		C^4=S	710	363.8	Yes
(5) 2-Thiouracil residue	300	C^2=S	717	300, 390	(Yes)
		C^4=O	1690	300, 290	Yes
(6) Guanine residue	276, 250	C=O	1710	257.3	No
(7) Cytosine residue	268	C=O	1652	257.3	Yes
(8) NMN (NAD)	265	C=O	1660*	300	No
(9) NADH	340	C=O	1693	351.1	Yes
(10) FAD (FMN)†	448	C^2=O	1640‡	363.8	No
	374	C^4=O	1701	363.8	No
(11) Actinomycin D	442	C=O	1656§	457.9	No

*From (*8*). †FAD, flavin adenine dinucleotide; FMN, flavine mononucleotide. ‡C=O stretching frequency observed in the infrared spectrum of FMN in D_2O by Abe and Kyogoku (*9*). §C=O stretching frequency observed in the infrared spectrum of 3-amino-1,8-dimethylphenoxazone by Musso and Matthies (*10*).

on C=O do not necessarily migrate into the main π-electron system, so that they do not necessarily participate in the $\pi\pi^*$ transition of the main conjugated system.

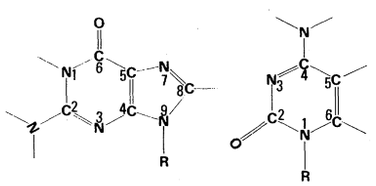

6 7

On the basis of the data given in Table 1, the carbonyl bond of the cytosine residue (**7**) must be involved in the conjugated system that is responsible for the 268-nm band. The C=O in the guanine residue (**6**), on the other hand, does not seem to be involved in the conjugated

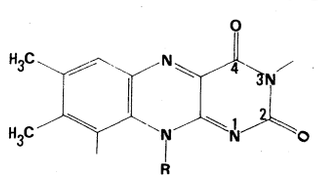

10

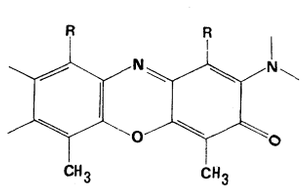

11

system; the main π-electrons probably go around C^8=N^7-C^5=C^4-N^3=C^2, which gives rise to the 276- and 250-nm bands. It is interesting that the C^2=S stretching Raman line (717 cm^{-1}) of the 2-thiouracil residue (**5**) appears weakly on excitation at 300 nm. Therefore the π-electrons on C^2=S must migrate into the O=C^4-C^5=C^6 system to some extent, in contrast to the uracil C^2=O, whose π-electrons do not seem to migrate into the O=C^4-C^5=C^6 system at all.

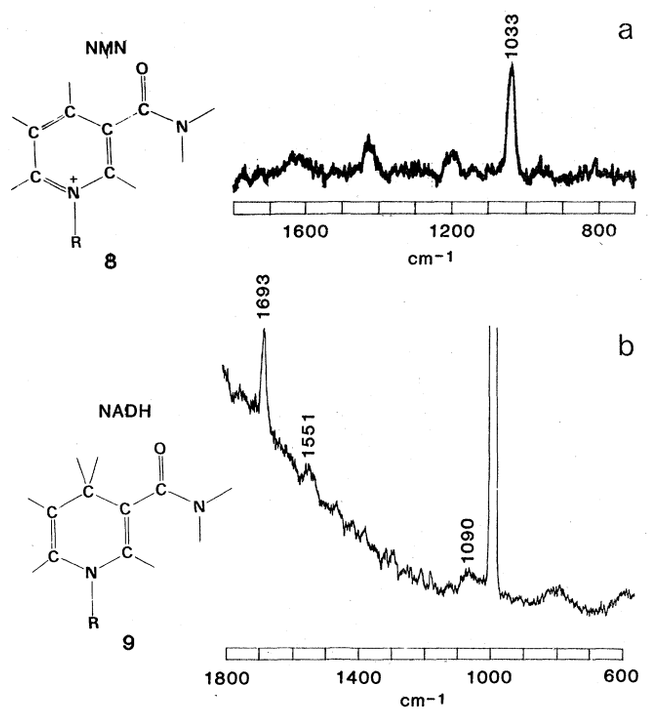

Fig. 1. Raman spectra of (a) NMN (**8**) and (b) NADH (**9**) in aqueous solution. In (b), the strong peak at 980 cm^{-1} is due to a natural emission of the Ar^+ laser used for excitation.

Nicotinamide mononucleotide (NMN) and nicotinamide adenine dinucleotide (NAD) have a ring system (**8**) that is similar to the pyridinium ring and has an absorption band at 265 nm. On excitation at 300 nm, the ring "breathing" line at 1033 cm^{-1} is found to be in resonance, but the C=O stretching line is not (Fig. 1a). When NAD is reduced to dihydronicotinamide adenine dinucleotide (NADH) (**9**), a new absorption band appears at 340 nm. The carbonyl stretching line at 1693 cm^{-1} is now found to be in resonance on excitation at 351.1 nm (Fig. 1b). Thus, the carbonyl bond is not involved in the conjugated double-bond system in **8**, but it is involved in **9**.

On the basis of our Raman spectroscopic studies with 363.8- and 457.9-nm excitation, the carbonyl bonds of flavin (**10**) and actinomycin D (**11**) are not considered to be involved in their conjugated double-bond systems, which are responsible for the absorption bands (Table 1).

YOSHIFUMI NISHIMURA
MASAMICHI TSUBOI
Faculty of Pharmaceutical Sciences, University of Tokyo, Hongo, Bunkyo-ku, Tokyo, Japan

References and Notes

1. A. Y. Hirakawa and M. Tsuboi, *Science* **188**, 359 (1975).
2. J. C. D. Brand and D. G. Williamson, *Discuss. Faraday Soc.* **35**, 184 (1963). However, one should consider possible lack of planarity of this molecule.
3. H. Hosoya, J. Tanaka, S. Nagakura, *Bull. Chem. Soc. Jpn.* **33**, 850 (1960).
4. T. Ishiguro, E. Suzuki, A. Y. Hirakawa, M. Tsuboi, *J. Mol. Spectrosc.*, in press.
5. Y. Nishimura, H. Haruyama, K. Nomura, A. Y. Hirakawa, M. Tsuboi, *Bull. Chem. Soc. Jpn.* **52**, 1340 (1979).
6. W. Hug and I. Tinoco, *J. Am. Chem. Soc.* **95**, 2803 (1979).
7. C. Nagata, A. Imamura, H. Fujita, *Advances in Biophysics*, M. Kotani, Ed. (Univ. of Tokyo Press, Tokyo, 1973), vol. 4, p. 1.
8. B. S. Yu, thesis, University of Tokyo (1970).
9. M. Abe and Y. Kyogoku, personal communication.
10. H. Musso and H. G. Matthies, *Chem. Ber.* **90**, 1814 (1957).

11. We thank H. Umezawa for the sample of actinomycin D and S. Higuchi for the sample of 1-cyclohexyl-2-thiouracil. We also thank Y. Kyogoku for providing his infrared data on flavine monomucleotide before publication. Part of our experiment was done in collaboration with K. Kawasaki. Partly supported by a grant-in-aid for Special Project Research from the Ministry of Education, Science, and Culture of Japan.

14 May 1980; revised 3 July 1980

Comparison of the Nucleic Acid Sequence of Anglerfish and Mammalian Insulin mRNA's from Cloned cDNA's

Abstract. *Anglerfish (*Lophius americanus*) insulin complementary DNA was cloned in bacterial plasmids, and its sequence was determined. Fish insulin messenger RNA is larger (1.5 times) than the messenger RNA encoding mammalian (rat and human) insulin, in part because of a larger C peptide (an additional six amino acids or 18 nucleotides in length) but mainly because of increases in the 5' and 3' untranslated regions. Comparison of the fish, rat, and human insulin messenger RNA (from the complementary DNA) reveals that, in addition to the regions coding for the A and B peptides, sequence conservation is limited to a segment within the 5' untranslated region which may be involved in ribosomal binding, two small segments of the signal peptide, and two stretches of sequence in the 3' untranslated region.*

The sequences of both the human and rat insulin messenger RNA's (mRNA), from complementary DNA's (cDNA) and genomic DNA fragments containing the insulin gene have been determined (*1*-*6*). We present here the sequence of anglerfish insulin cDNA and the predicted preproinsulin peptide which it encodes. This study allows a comparison of the structure of evolutionarily distant vertebrate insulin mRNA's in both the coding and noncoding regions.

Anglerfish was selected as a source of fish insulin mRNA because it has a large endocrine pancreas (Brockmann body) which can be freed of exocrine pancreatic tissue. The polyadenylated mRNA fraction was prepared from isolated Brockmann bodies; it is highly enriched with respect to two size classes of RNA (840 ± 25 and 700 ± 25 bases) (Fig. 1, lane 2). Since insulin is a major product of Brockmann body tissue (*7*) we expected that insulin mRNA might be present in one of the frequent RNA size classes. A cDNA library was constructed from total Brockmann body polyadenylated RNA and single-stranded cDNA synthesized from the same RNA was used to screen the clones. The details of the cloning procedure have been described (*8*). This screening resulted in the identification of three major cDNA families. Two of the families hybridized to mRNA's in the 700-base size class and have been shown to encode peptide sequences for distinct somatostatins (somatostatin I and somatostatin II) (*8*). The other family, containing the most frequent cDNA's, hybridized to the 840-base mRNA as shown in Fig. 1, lane 3. Three plasmids from this family containing overlapping inserts (pLaI-1, -2, -3) were mapped and sequenced (Fig. 2). Together they comprise 657 bases of the 840-base mRNA.

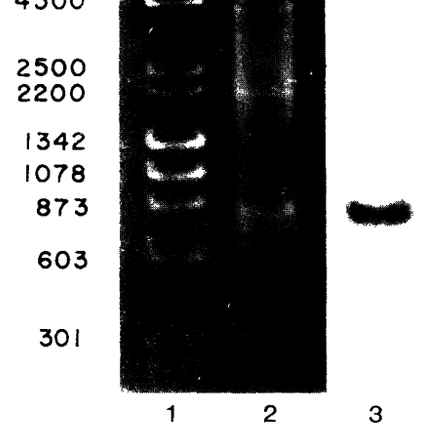

Fig. 1. Size determination of anglerfish insulin mRNA. Brockmann body polyadenylated mRNA was isolated and fractionated (*8*), placed on a 1.5 percent agarose gel containing 4 m*M* methyl mercury, and subjected to electrophoresis for 12 hours at 20 V (*22*). The stained and photographed gel was then "blotted" on diazotized paper (12 hours at room temperature) (*23*) and subsequently hybridized (*8*) at 42°C (for 48 hours) to a cloned insulin cDNA fragment (pLaI-2) labeled with ^{32}P by nick translation (*24*). (Lane 1) DNA molecular weight standards consisting of Hind III-digested lambda phage and Hae III-digested $\phi\chi$174. (Lane 2) Ethidium bromide stain of 1 μg of Brockmann body polyadenylated RNA. (Large molecular weight bands represent ribosomal RNA contaminants of the polyadenylated mRNA fraction.) (Lane 3) Autoradiograph of lane 2 RNA hybridized to the pLaI-2 probe.

Translation of the mRNA (the cDNA strand with a stretch of A's at its 3' end) beginning at the first AUG (A, adenine; U, uracil; G, guanine) codon predicts the amino acid sequence of a 12,730-dalton peptide, which we identify as anglerfish preproinsulin (Fig. 3). The precursor contains a signal peptide of 24 amino acids preceding a proinsulin moiety comprising insulin B and A chains and a connecting peptide of 41 amino acids. The amino acid sequences of the A and B chains predicted from the nucleic acid sequence are identical with those previously determined by amino acid sequence analysis (*9*). The predicted sequence of the signal peptide has been confirmed by Shields (*10*). The molecular weight of preproinsulin is slightly larger than that estimated for an immunoprecipitable peptide synthesized in vitro from anglerfish polyadenylated mRNA (*7*).

The anglerfish preproinsulin signal peptide, like those of other secretory proteins, contains a cluster of hydrophobic amino acid residues. Whereas the first 17 amino acids of the human and rat insulin peptides are highly conserved (Fig. 4), there is much less homology evident in the fish signal peptide. However, two regions have been conserved between fish and mammals—the Ala-Leu-Trp close to the initiating methionine and the hydrophobic Leu-Leu (Ala or Val) Leu-Leu (Fig. 4). These conserved sequences may have a specific function in the vectorial transport process.

The amino acid sequence of the anglerfish B and A chains is strongly homologous to other B and A chains including those from mammals. In contrast, the C peptide is 41 amino acids in length; this compares with 35 for rat and human (including the connecting basic residues at each end of the C peptide). This is the largest connecting peptide yet found for any insulin precursor. It bears little resemblance to that of mammals, supporting the belief that it functions only to allow the correct folding of the proinsulin prior to processing. As in all oth-

0036-8075/80/1219-1360$00.50/0